The serum protein renalase reduces injury in experimental pancreatitis

Received for publication, April 5, 2017, and in revised form, October 12, 2017 Published, Papers in Press, October 17, 2017, DOI 10.1074/jbc.M117.789776

Thomas R. Kolodecik[‡§], Anamika M. Reed[‡§], Kimie Date[¶], Christine A. Shugrue[‡§], Vikhil Patel[‡§], Shang-Lin Chung[‡§], Gary V. Desir[‡§1], and Fred S. Gorelick[‡§1,2]

From the [‡]Yale University School of Medicine, New Haven, Connecticut 06510, [§]Veterans Affairs Connecticut Healthcare System, West Haven, Connecticut 06516, and [¶]Ochanomizu University, Tokyo 112-8610, Japan

Edited by Henrik G. Dohlman

Acute pancreatitis is a disease associated with inflammation and tissue damage. One protein that protects against acute injury, including ischemic injury to both the kidney and heart, is renalase, which is secreted into the blood by the kidney and other tissues. However, whether renalase reduces acute injury associated with pancreatitis is unknown. Here, we used both *in vitro* and *in vivo* murine models of acute pancreatitis to study renalase's effects on this condition. In isolated pancreatic lobules, pretreatment with recombinant human renalase (rRNLS) blocked zymogen activation caused by cerulein, carbachol, and a bile acid. Renalase also blocked cerulein-induced cell injury and histological changes. In the *in vivo* cerulein model of pancreatitis, genetic deletion of renalase resulted in more severe disease, and administering rRNLS to cerulein-exposed WT mice after pancreatitis onset was protective. Because pathological increases in acinar cell cytosolic calcium levels are central to the initiation of acute pancreatitis, we also investigated whether rRNLS could function through its binding protein, plasma membrane calcium ATPase 4b (PMCA4b), which excretes calcium from cells. We found that PMCA4b is expressed in both murine and human acinar cells and that a PMCA4b-selective inhibitor worsens pancreatitis-induced injury and blocks the protective effects of rRNLS. These findings suggest that renalase is a protective plasma protein that reduces acinar cell injury through a plasma membrane calcium ATPase. Because exogenous rRNLS reduces the severity of acute pancreatitis, it has potential as a therapeutic agent.

Acute pancreatitis is a potentially life-threatening disease that affects more than 250,000 people each year in the United States, making it the leading cause of hospitalization for gastrointestinal disorders (1). In those with severe disease, mortality rates of 10–30% are reported. The mainstay of treatment is supportive care, a fact that likely relates to our limited understanding of the pathogenesis of acute pancreatitis.

A number of injurious factors can contribute to the initiation and progression of acute pancreatitis. The pancreatic acinar cell is held to be the most likely site of disease initiation. One of the earliest and most studied responses in acute pancreatitis are changes in acinar cell cytosolic calcium $[Ca^{2+}]_i$ signaling (2). Physiologic stimulation results in an oscillatory response in $[Ca^{2+}]_i$. During pathologic stimulation, this oscillatory response is replaced by a much higher non-oscillatory $[Ca^{2+}]_i$ spike that remains above baseline levels for a prolonged time. Other important early pancreatitis responses that can influence the onset and severity of this disease include activation of digestive enzymes in the acinar cell, up-regulation of inflammatory responses, and enhanced vascular permeability. Although the list of damaging factors is extensive and includes IL1, IL6, TNFα, and platelet-activating factor, less is known about endogenous factors that can limit disease severity.

In a search for factors that might mediate the clinical effects of renal failure, the serum protein renalase (RNLS)[3] was discovered (3). This secretory protein is primarily made by the kidney but is also synthesized in other tissues and disappears from the serum during chronic renal failure. Administration of exogenous recombinant RNLS (rRNLS) reverses some of the complications of experimental chronic renal failure and reduces acute oxidative renal injury (4). This protective effect on acute injury was independent of RNLS's NADH oxidase activity. We have subsequently found that RNLS functions as a prosurvival factor both *in vitro* and *in vivo* in the context of malignancy (5, 6). This effect appears to be mediated by selective binding of RNLS to a plasma membrane calcium ATPase (PMCA), most likely the PMCA4b isoform (7). We have shown that oxidant injury to cultured renal cells can be reduced by RNLS stimulation of PMCA (7). Thus, in cultured cells, RNLS binding to PMCA4b mediates its survival effects; the PMCA inhibitor caloxin and an siRNA specific for PMCA4b both block the RNLS protective effects (7).

This study examines the potential role of RNLS using a standard experimental model of cerulein-induced pancreatitis in

This work was supported by NIDDK, National Institutes of Health Grants DK007356, DK034989, DK086465, DK086402, and DK081037 (to G. V. D.) and K08 DK007356 (to A. R.); Japan Society for the Promotion of Science Grant 40058 (to K. D.); a United States Department of Veterans Affairs merit award (to F. S. G.); and a Howard Hughes Medical Institute student fellowship (to S. C.). G. V. Desir is a named inventor on several issued patents related to the discovery and therapeutic use of renalase. Renalase is licensed to Bessor Pharma, and G. V. Desir holds an equity position in Bessor and its subsidiary Personal Therapeutics. The content is solely the responsibility of the authors and does not necessarily represent the official views of the National Institutes of Health.

[1] Both authors contributed equally to this work.

[2] To whom correspondence should be addressed: Dept. of Internal Medicine and Cell Biology, VA CT Healthcare System and Yale University School of Medicine, 950 Campbell Ave., West Haven, CT 06516-2700. Tel.: 203-932-5711 (ext. 3679); E-mail: fred.gorelick@yale.edu.

[3] The abbreviations used are: RNLS, renalase; rRNLS, recombinant human renalase; PMCA, plasma membrane calcium ATPase; CER, cerulein; MTT, 3-(4,5-dimethylthiazol-2-yl)-2,5-diphenyltetrazolium bromide; TLCS, taurolithocholic acid sulfate; IF, immunofluorescence.

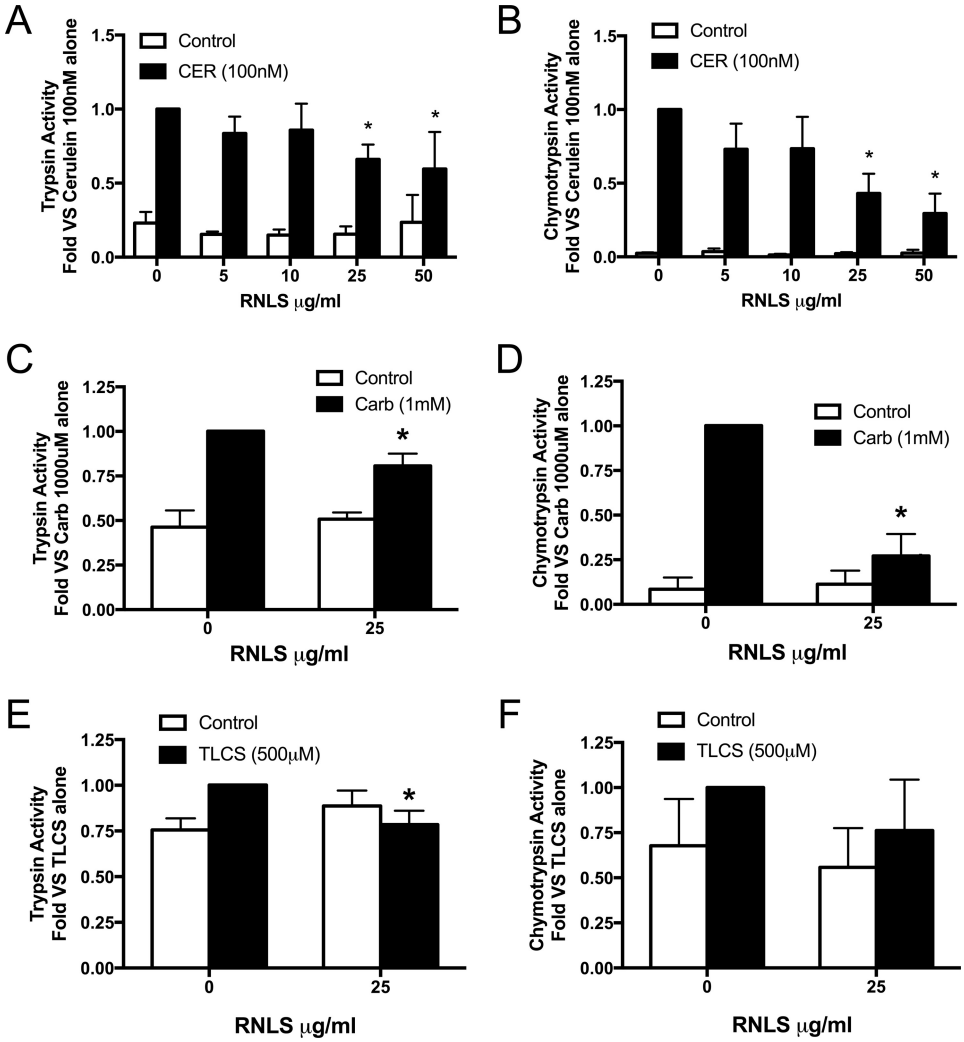

Figure 1. RNLS decreases secretagogue-stimulated zymogen activation in pancreatic lobules. The concentration dependence of rRNLS on CER-stimulated zymogen activation in pancreatic lobules was examined with or without recombinant RNLS (5–25 μg/ml) for 30 min prior to addition of either medium or cerulein (100 nM) for 30 min, and trypsin (*A*) and chymotrypsin (*B*) activities were measured. The effects of RNLS (25 μg/ml) on carbachol (*Carb*) (1 mM) or TLCS (500 μM) added to cells after RNLS treatment for 30 min were examine, and trypsin (*C*, carbachol; *E*, TLCS) and chymotrypsin (*D*, carbachol; *F*, TLCS) activities were assayed. *, $p < 0.05$ compared with cerulein, carbachol, or TLCS alone. For cerulein, $n = 7$ studies ($n = 3$ studies for 50 μg/ml RNLS); for carbachol, $n = 4$ studies; for TLCS, $n = 5$ studies. Values represent the mean, and *error bars* represent the S.E.

the mouse. Cerulein (CER) is an orthologue of the mammalian hormone cholecystokinin. When given at concentrations 10-100-fold greater than physiologic levels, cerulein reproducibly causes an edematous and non-lethal form of acute pancreatitis. In acinar cells, we found that rRNLS reduced cerulein-induced injury. In a mouse with genetic deletion of RNLS, cerulein-induced pancreatitis was worse than that seen in wild-type (WT) mice. Administering exogenous rRNLS after the induction of cerulein pancreatitis reduced disease severity. These protective effects of renalase are likely related, at least in part, to activation of plasma membrane calcium ATPase. These results provide a basis for further investigation into RNLS as a potential treatment for pancreatitis.

Results

Renalase pretreatment decreases pancreatitis responses in isolated pancreatic tissue

The potential protective effects of renalase were first examined in pancreatic lobules exposed to agents that elicited early pancreatitis responses in acinar cells. Lobules treated with secretagogues showed variation in both basal and stimulated zymogen activation among experiments but had the same pattern of activation. For this reason, data are presented as -fold *versus* maximal response. We observed that the effects of rRNLS on CER-stimulated zymogen activation was concentration-dependent, inhibiting both trypsinogen (Fig. 1*A*) and chymotrypsinogen activation (Fig. 1*B*) with 25 μg/ml or higher RNLS having a significant effect. For all subsequent experiments, a dose of 25 μg/ml was used. rRNLS also inhibited carbachol (a muscarinic receptor agonist)-stimulated trypsinogen (Fig. 1*C*) and chymotrypsinogen activation (Fig. 1*D*) and tended to have similar protective effects after bile acid exposure (Fig. 1, *E* and *F*). rRNLS significantly reduced cellular injury as measured by MTT conversion, a measure of metabolic function, in CER-treated lobules (Fig. 2*A*). rRNLS also prevented morphologic changes in acinar cells associated with pancreatitis; most notably, the typical acinar cell vacuolization was eliminated (Fig. 2*B*, compare *panel 2 versus panel 4*). These observations

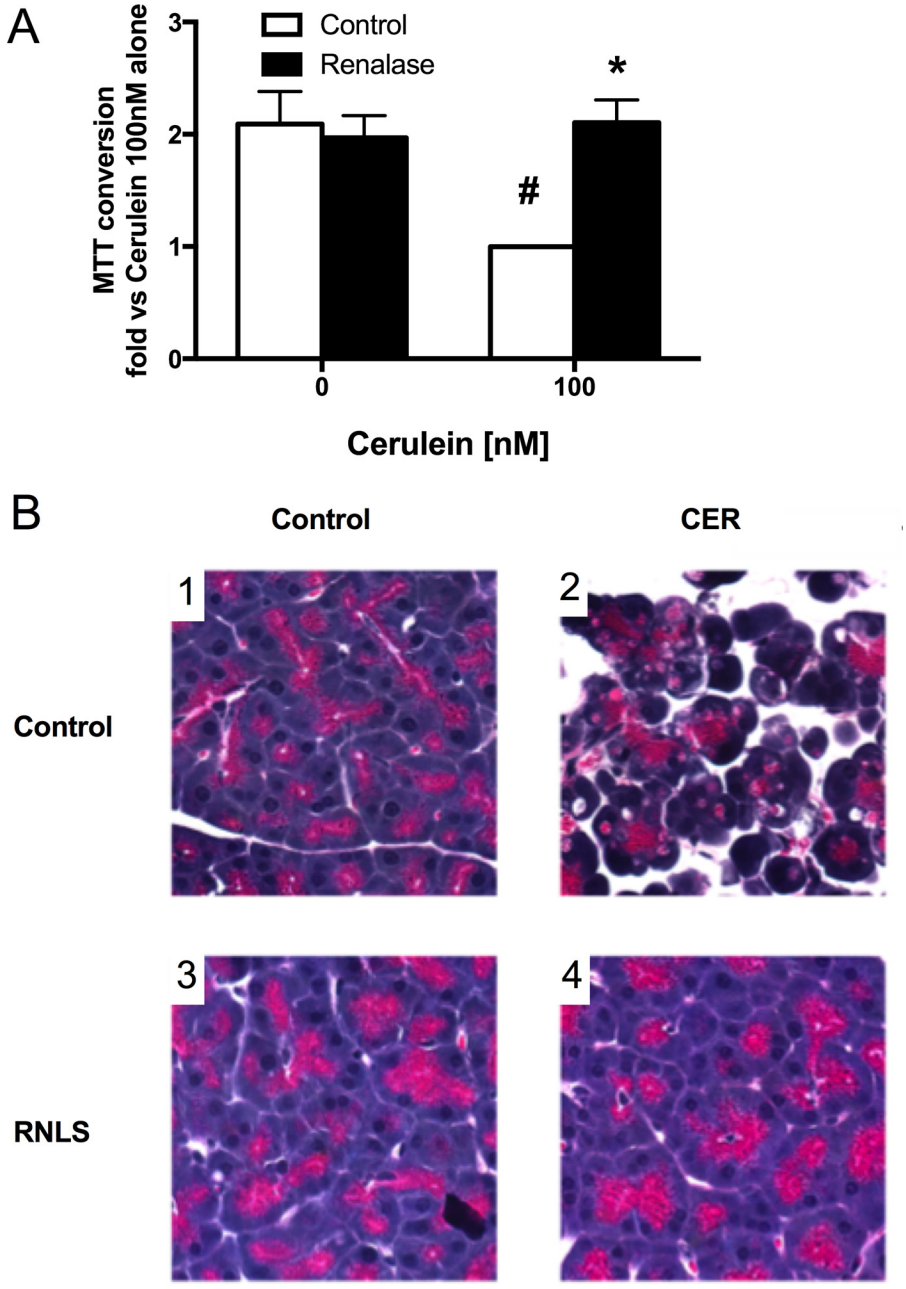

Figure 2. RNLS reduces injury in pancreatic lobules. Pancreatic lobules were preincubated with RNLS (25 μg/ml) for 30 min prior to CER (100 nM) administration to induce pancreatitis responses. Markers of cellular injury were assayed. *A*, MTT conversion. *B*, *panels 1–4*, pancreatic histology (H&E staining; photos taken at 400×). #, $p < 0.05$ *versus* control; *, $p < 0.05$ *versus* CER alone. For MTT, $n = 4$ studies; for histology, $n = 3$ studies. Values represent the mean, and *error bars* represent the S.E.

provide evidence that RNLS can directly act on the pancreatic acinar cell to reduce pancreatitis injury. We next examined the effects of pancreatitis on plasma RNLS levels.

Induction of pancreatitis decreases serum renalase levels, which return to baseline prior to recovery from pancreatitis

Within 15 min of inducing CER pancreatitis, plasma RNLS levels were reduced; the lowest value was reached by 1 h (Fig. 3*A*). Levels remained low during the entire 6-h course of treatment but returned to control levels 6 h after CER treatment stopped (at 12 h). Markers of pancreatitis such as serum amylase (Fig. 3*B*) and tissue edema (Fig. 3*C*) returned to control levels by 24 h after the initiation of pancreatitis. Thus, return of plasma RNLS to control values appears to precede other parameters of pancreatitis recovery.

Genetic deletion of renalase (KO) increases pancreatitis in vivo

The effects of endogenous RNLS in control conditions and on the severity of CER pancreatitis (7 h after induction) were examined in mice with a pan-deletion of RNLS. This genetic model was developed in our laboratory and its primary phenotype is mild hypertension (8). No overt differences were seen in baseline responses (data not shown). After induction of CER pancreatitis, we found that RNLS deletion did not change either

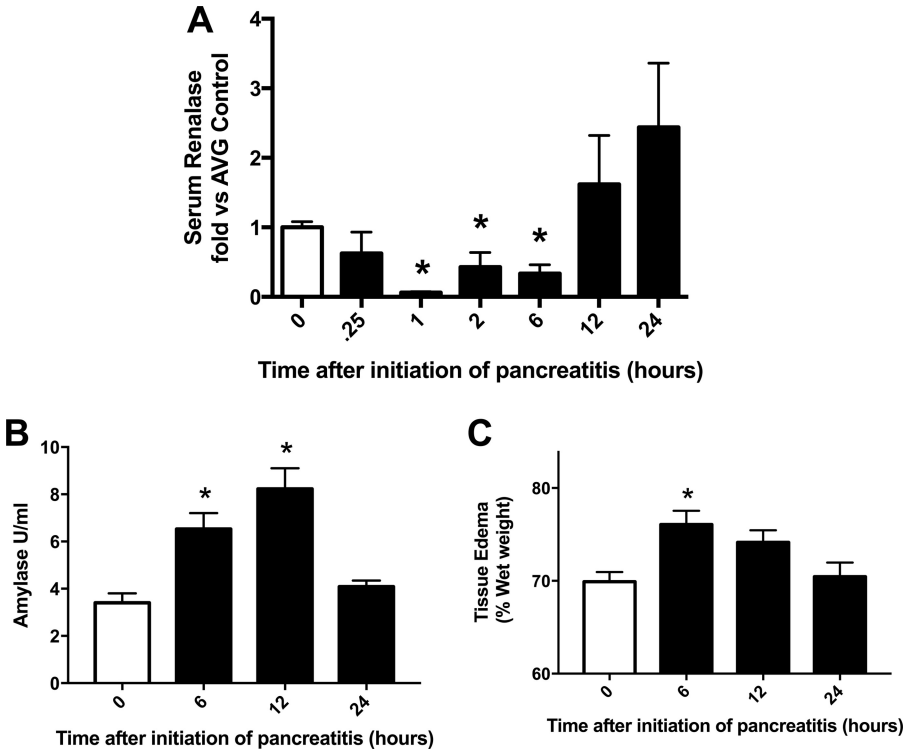

Figure 3. Plasma RNLS levels drop dramatically with CER stimulation *in vivo*. Pancreatitis was induced in mice by six hourly injections of CER (50 μg/kg of body weight). At the indicated times after the first CER injection, plasma and pancreas were collected for determination of plasma RNLS levels by immunoblot analysis (*A*), plasma amylase levels (*B*), and tissue edema as determined by wet *versus* dry weight (*C*). *White bars* are control, which received only PBS. *Black bars* are CER-treated. *, $p < 0.05$ compared with PBS (*white bar*). $n = 5$ or more for each time point. Values represent the mean, and *error bars* represent the S.E. *AVG*, average.

tissue edema (percent wet weight) or serum amylase levels (data not shown). Some histological features of CER-induced pancreatitis were worse in RNLS knock-out mice, including edema and macrophage infiltration, but not neutrophil infiltration or vacuolization, and the number of pyknotic nuclei decreased (Fig. 4). These findings suggest that genetic deletion of RNLS worsens select early parameters of CER-induced pancreatitis compared with WT. We next determined whether exogenous RNLS could reduce the severity of CER-induced pancreatitis.

Effects of renalase after the onset pancreatitis

To better reflect the clinical presentation in which most pancreatitis patients are seen after disease onset, rRNLS was given after disease onset in our experimental model. rRNLS administration did not affect baseline parameters such as tissue edema (by percent wet weight) or serum amylase (data not shown). However, CER pancreatitis was much less severe histologically (Fig. 5). This included less morphologic edema (Fig. 5*E*), fewer vacuoles (Fig. 5*F*), and a significant decrease in neutrophil infiltration (Fig. 5*H*). Together, these findings suggest that RNLS has protective effects in cellular and *in vivo* models of acute experimental pancreatitis. Because other studies from our group have suggested that RNLS may act through a plasma membrane calcium ATPase, we investigated whether this could also be a target in the pancreas (7).

PMCA gene expression in pancreatic acinar cells

We recently used photoaffinity cross-linking to identify plasma membrane RNLS-binding proteins; the PMCA type 1 and 4b isoforms were identified (7). Genetic down-regulation of PMCA4b was shown to eliminate the protective effect of RNLS in cultured cells (7). To determine whether such transporters were encoded for in the pancreatic acinar cell, we used polymerase chain reaction (PCR) analysis and PMCA isoform–specific primers. Mouse brain, which contains all major PMCA isoforms, was used as a positive control. Murine pancreatic acinar cells showed transcripts for PMCA1, -2, and -4. PMCA4 has two splice variants, PMCA4a and PMCA4b; only PMCA4b was found in acinar cells (Fig. 6*A*). In human pancreatic acinar cells, PMCA1 and -4b were highly expressed (Fig. 6*B*). We next examined the localization of PMCA4 in acinar cells.

Localization of PMCA4b in pancreatic lobules

To determine the distribution of PMCA4b in pancreatic tissue, we double labeled control pancreas with an antibody specific for PMCA4b (JA-3) and phalloidin, which labels apical F-actin bundles in the acinar cell. We found that PMCA4b primarily had a predominately basal distribution and did not colocalize with phalloidin staining (Fig. 6). This distribution is consistent with a basolateral localization of the transporter in most other epithelial cells, although an apical distribution has been reported in the parotid acinar cell (9, 10). Whether PMCA could mediate the effects of RNLS in the acinar cell was next investigated using an inhibitor of PMCA and examining the effects of RNLS on secretagogue-stimulated zymogen activation and cellular injury.

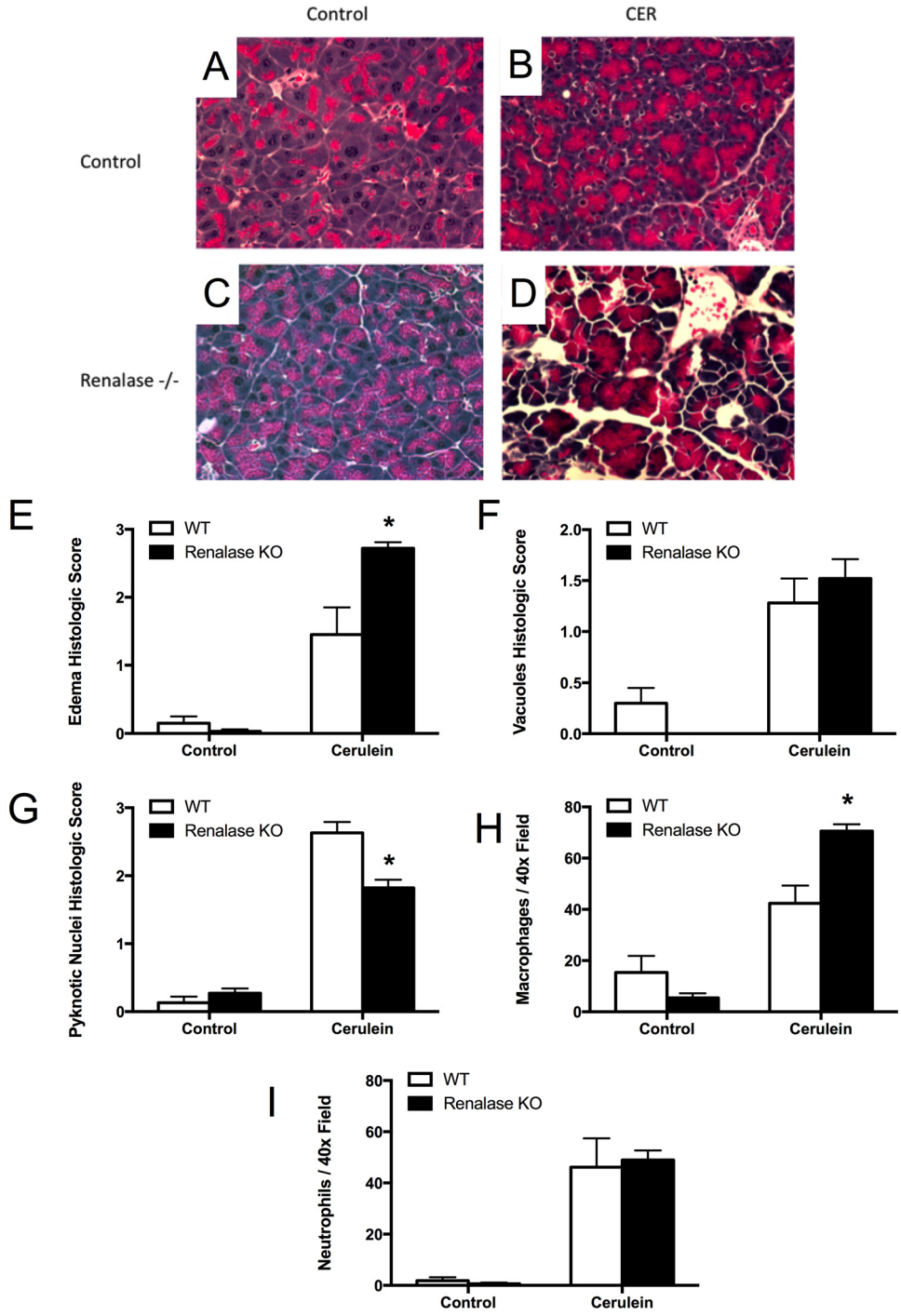

Figure 4. Genetic deletion of RNLS *in vivo* causes an increase in cerulein-stimulated histological damage *in vivo*. WT or RNLS KO (renalase $^{-/-}$) animals were given six hourly injections of either PBS as a control or cerulein (50 μg/kg) to induce pancreatitis. Tissues were fixed in buffered formalin and stained with H&E. *A*, WT control. *B*, WT cerulein. *C*, RNLS$^{-/-}$. D, RNLS$^{-/-}$ + cerulein. Slides were examined, and sections were randomly photographed at 400×. Slides were scored in a blinded manner for histologic markers of pancreatitis based on previously published criteria (22, 27). Markers examined included edema (*E*), intracellular vacuoles (*F*), pyknotic nuclei and apoptotic bodies (*G*), macrophages (*H*), and neutrophils (*I*). *, $p < 0.05$ compared with analogous WT cerulein. $n = 3$ for each treatment group. Values represent the mean, and *error bars* represent the S.E.

A PMCA inhibitor blocks the protective effect of renalase on secretagogue-stimulated pancreatitis in pancreatic lobules

To determine whether PMCA was involved in the protective effects of RNLS, we used caloxin 1b1, a peptide inhibitor that exhibits selectivity for PMCA4a and PMCA4b. We preincubated pancreatic lobules with caloxin 1b1 (100 μM) for 30 min prior to the addition of RNLS followed by CER stimulation. As shown in Fig. 7, we found that caloxin 1b1 pretreatment had no significant effect on basal zymogen activation (Fig. 7, *A* and *B*) or amylase secretion (Fig. 7*C*). However, it blocked the protective effect of renalase on CER (100 nM)-stimulated trypsinogen (Fig. 7*A*) and chymotrypsin (Fig. 7*B*) activation. Caloxin 1b1 pretreatment reversed the decrease in CER-stimulated amylase secretion seen with RNLS (Fig. 7*C*). Interestingly, caloxin

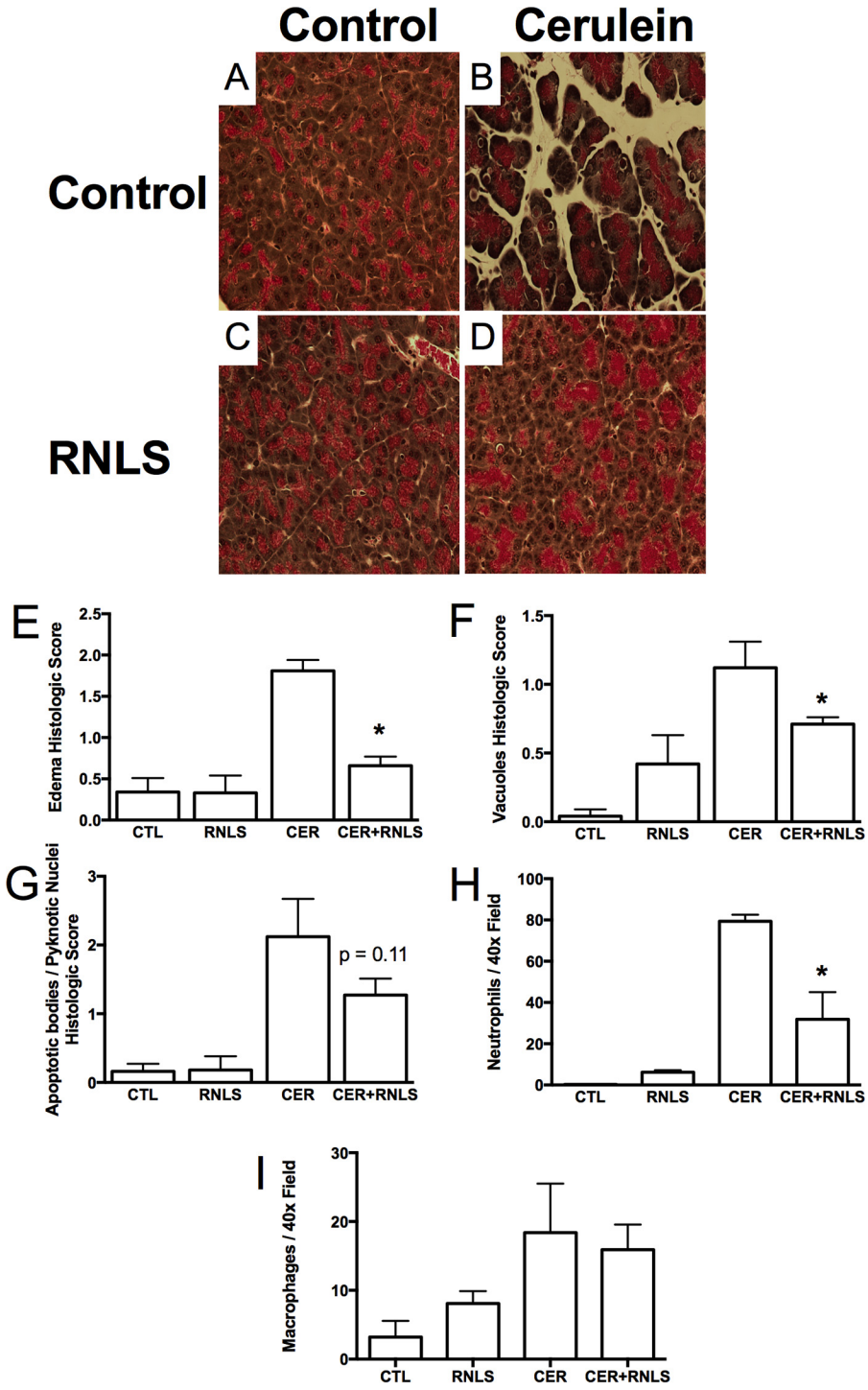

Figure 5. RNLS administration after the induction of cerulein pancreatitis decreases histologic changes associated with cerulein pancreatitis. WT mice were given six hourly injections of either PBS as a control or cerulein (50 μg/kg) to induce pancreatitis. Concurrent with the third cerulein injection, RNLS (4 mg/kg) was given to half of the animals in each group, and PBS was given to the other half. Tissues were fixed in buffered formalin and stained with H&E. *A*, control (*CTL*). *B*, cerulein. *C*, RNLS (*REN*) alone. *D*, RNLS after cerulein. Stained slides were examined, and random fields were photographed at 400×. Sections were scored in a blinded manner for histologic markers of pancreatitis, including edema (*E*), intracellular vacuoles (*F*), pyknotic nuclei and apoptotic bodies (*G*), neutrophils (*H*), and macrophages (*I*). *, $p < 0.05$ compared with cerulein alone. $n = 4$ for each treatment group. Values represent the mean, and *error bars* represent the S.E.

tended to enhance CER (100 nM)-stimulated zymogen activation when RNLS was not present. To further examine the effect of caloxin 1b1 on zymogen activation, we pretreated lobules with caloxin with or without various concentrations of CER (Fig. 8, *A* and *B*). Caloxin 1b1 tended to enhance both basal and CER-stimulated trypsin activation (Fig. 8*A*). Although the same pattern was seen for chymotrypsin, the changes were not significant (Fig. 8*B*). Similar results for caloxin 1b1 sensitization were seen with trypsinogen (Fig. 8*C*) and chymotrypsinogen (Fig. 8*D*) activation in response to carbachol. The effects of

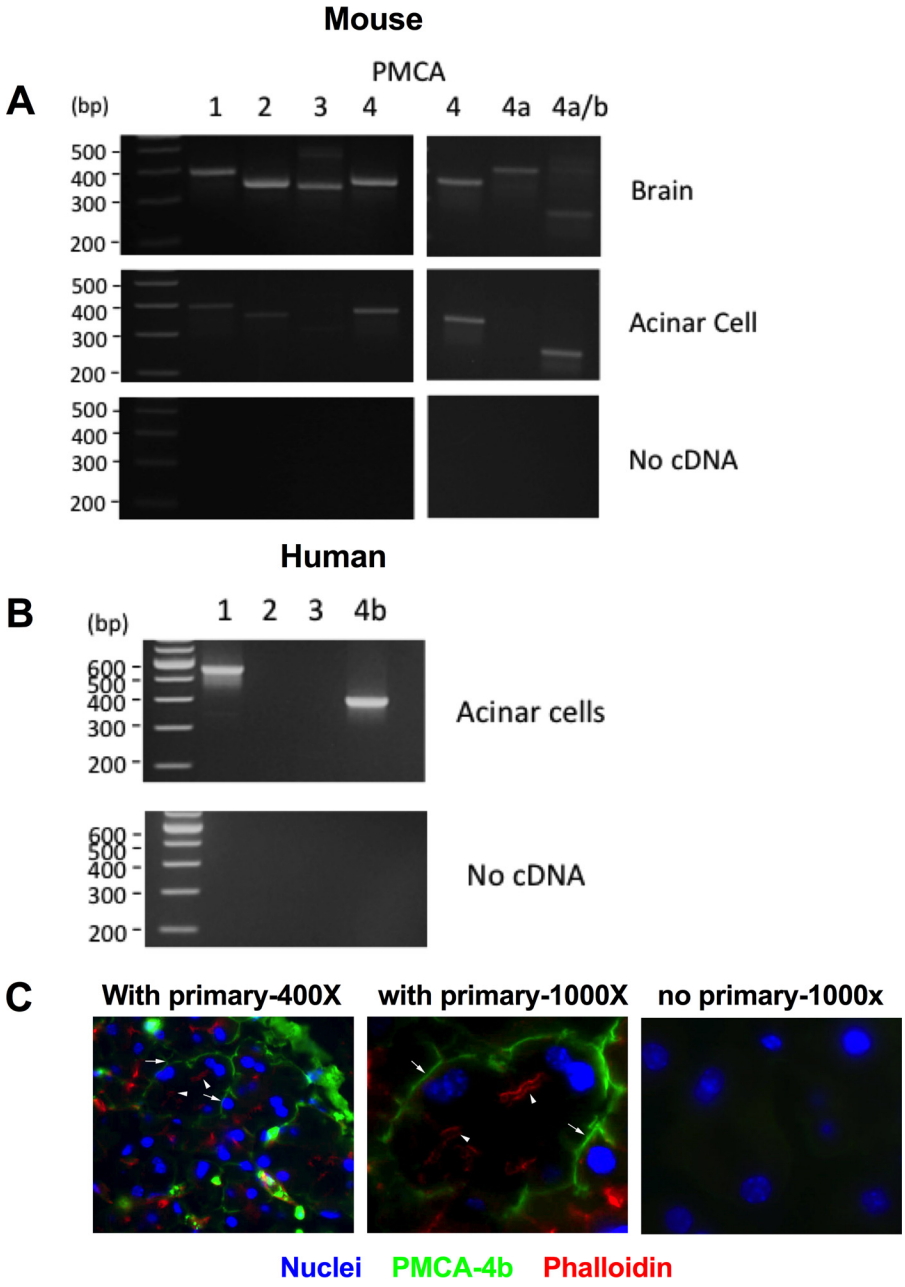

Figure 6. PMCA isoforms are expressed in the pancreatic acinar cell. RNA was isolated from both mouse and human pancreatic acinar cells as well as whole brain as a positive control. First-strand cDNA was generated and used as a template for PCRs. Specific primers were used for the different PMCA isoforms. A, mouse. *B*, human. PMCA4b was also localized to the basal/lateral membrane of pancreatic acinar cells by immunofluorescence. *C*, representative image of pancreatic tissue labeled for PMCA4b (*green*), actin (phalloidin; *red*), and nuclei (DAPI; *blue*). Photomicrographs were taken at 400× or 1000× *magnification*. *Arrowheads* indicate apical actin staining, and *arrows* indicate predominately basal PMCA4b labeling.

RNLS on cell injury were then evaluated. As shown in Fig. 9, pretreatment with caloxin 1b1 blocked the protective effects of RNLS after CER hyperstimulation as measured by the MTT assay of metabolic function. Although caloxin alone enhanced cell injury, it did not increase injury induced by supraphysiologic CER. Caloxin alone had no effect on injury associated with lower doses of CER (data not shown). Lastly, caloxin alone did not cause intracellular vacuole formation as is seen in CER treatment (data not shown). Together, these studies suggest that the protective effects of RNLS on CER-induced acinar cell injury are mediated by a PMCA. Based on our previous studies using affinity cross-linking to identify RNLS-binding proteins and knockdown studies in other cell types, these effects are likely mediated by PMCA4b.

Discussion

Here, we examine whether RNLS, a plasma protein with protective effects in models of acute renal and cardiac injury (11, 12), could decrease injury in murine models of acute pancreatitis and whether it can act directly on the pancreatic acinar cell. Using the standard cellular and *in vivo* models of cerulein-induced acute pancreatitis, we observed a protective effect of RNLS. This included the effects of rRNLS on injuries generated by CER, carbachol, and bile acids on isolated groups of acinar cells. Global

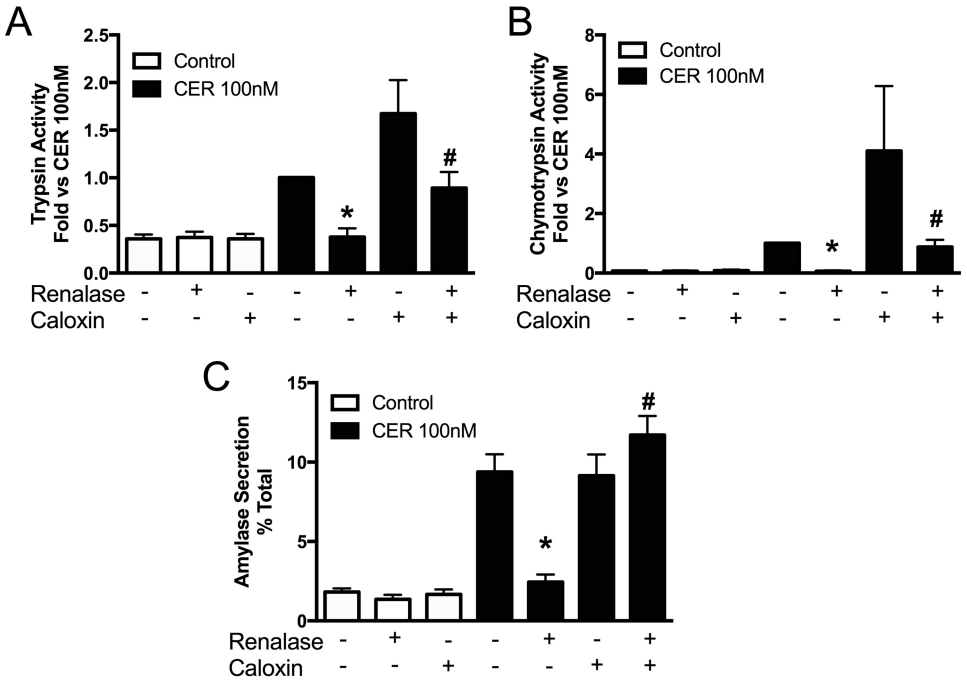

Figure 7. Caloxin blocks RNLS's protective effects against CER-induced zymogen activation and amylase secretion. Pancreatic lobules were treated with or without caloxin 1b1 (100 μM) for 30 min before the addition of RNLS (25 μg/ml). After 30 min of RNLS treatment, pancreatitis was induced in some lobules by the addition of CER (100 nM) for 30 min. Assays for zymogen activation (*A*, trypsin; *B*, chymotrypsin) and amylase secretion (*C*) were performed. *, $p < 0.05$ *versus* CER alone; #, $p < 0.05$ *versus* CER + renalase. For trypsin activation, chymotrypsin activation, and amylase secretion, $n = 4$ or more. Values represent the mean, and *error bars* represent the S.E.

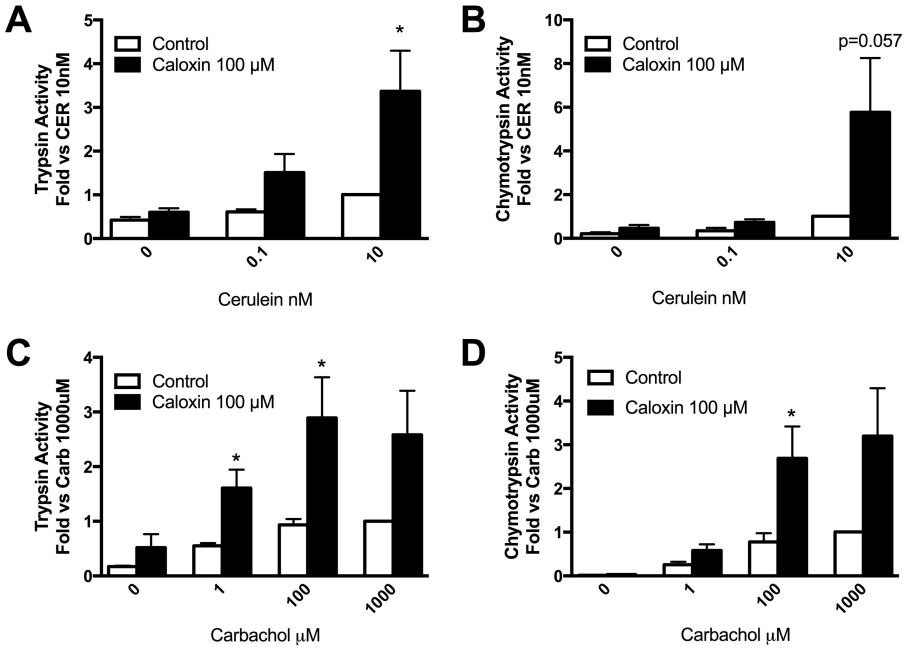

Figure 8. Inhibition of PMCA4 by caloxin 1b1 enhances CER- and carbachol-induced zymogen over a range of doses. Pancreatic lobules were isolated and pretreated with caloxin 1b1 (100 μM) for 30 min prior to treatment with either CER (0.1 or 10 nM) or carbachol (1, 100, or 1000 μM). Samples were assayed for trypsin (*A*, CER; *C*, carbachol (*Carb*)) and chymotrypsin (*B*, CER; *D*, carbachol) activities. *, $p < 0.05$ *versus* same treatment without caloxin 1b1. $n \geq 3$ for each experiment. Values represent the mean, and *error bars* represent the S.E.

deletion of RNLS in mice also resulted in more injury in the CER model, whereas administration of recombinant RNLS to WT mice reduced the severity of acute pancreatitis. When pancreatitis was induced by CER treatment, there was a rapid decrease in plasma renalase levels, reaching a nadir by 1 h. A low level of plasma RNLS persisted until 6 h when CER treatment ended; after 12 h, plasma RNLS levels returned to or exceeded baseline levels. The recovery of plasma renalase at 12 h preceded the resolution of pancreatitis, including increased pancreatic edema and serum amylase, which only normalized 24 h after the onset of injury. It may be that the return of plasma renalase levels to normal played a role in disease resolution.

Circulating RNLS may target multiple resident cell types within the pancreas, including endothelial cells, duct cells, islet

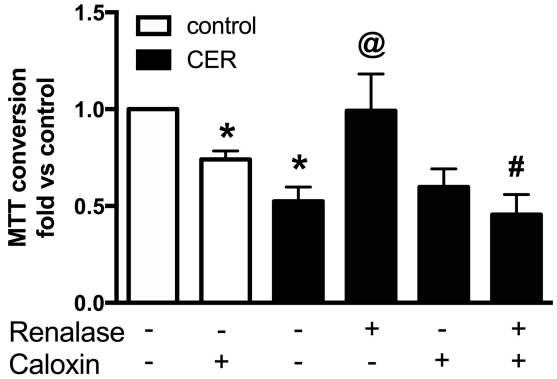

Figure 9. The effects of caloxin 1b1 treatment on cell injury in pancreatic lobules. We determine whether caloxin 1b1 could reverse the protective effect RNLS pretreatment had against CER (100 nM)-induced injury (MTT assay). Lobules were pretreated with caloxin 1b1 (100 μM) for 30 min followed by 30-min treatment with RNLS (25 μg/ml) and finally stimulation with CER (100 nM) for 90 min. Injury was then assessed by MTT assay. *, $p < 0.05$ *versus* control; @, $p < 0.05$ *versus* CER alone; #, $p < 0.05$ *versus* CER + renalase. $n \geq 3$. Values represent the mean, and *error bars* represent the S.E.

cells, and (as our data suggest) pancreatic acinar cells. Effects of RNLS on inflammatory cells, especially macrophages, are also likely. We recently reported that tumor-resident macrophages express high levels of RNLS and that this is associated with the macrophages having an anti-inflammatory M2 phenotype (6). M2 macrophages are associated with wound healing, tissue repair, and tumor promotion. In the context of cancer, we have suggested that dysregulated RNLS signaling could bias macrophages to an M2-like phenotype (13). We have also found that RNLS suppresses inflammasome activity in stimulated macrophages.[4] These findings are consistent with RNLS acting to suppress acute inflammatory responses. The plasma membrane ATPase PMCA4b has been identified as a receptor for renalase (7). Macrophages have been found to express PMCA4 (14). Studies are underway to examine the role of RNLS in macrophage responses in pancreatitis; we believe that RNLS will be found to have a role in modulating acute inflammation as well as resolution of this disease.

Previous studies have implicated PMCA in acute pancreatic acinar cell injury. In a study of oxidant stress induced by H_2O_2, complex concentration-dependent effects on acinar cell Ca^{2+} signaling and PMCA activity were observed (15). The authors concluded that, under control conditions, Ca^{2+} extrusion through PMCA was the major pathway for lowering cytosolic Ca^{2+}. Noting that insulin appears to have a protective role in models of exocrine pancreatic injury, its effects were examined in the setting of acinar cell oxidant-induced injury (16). In this study, insulin was found to substantially reduce acinar cell injury, increase PMCA-dependent Ca^{2+} extrusion, and reverse oxidant-dependent PMCA inhibition. Finally, in a pancreatic acinar cell model thought to simulate the oxidative conditions that cause alcohol- and fatty acid–related acute pancreatitis, insulin was shown to be protective and reduce Ca^{2+} overload through activation of PMCA (17). This study concluded that the effects of insulin on PMCA activities were through PI3K/Akt–dependent mechanisms that preserve ATP levels as well as unidentified PI3K/Akt–independent mechanisms. Together with the findings of this study, we conclude that PMCA activation can reduce acinar cell pancreatitis injury (7). However, the present study provides three important advances. First, unlike insulin, it reports that activation of PMCA by a ligand that likely binds its extracellular domain (RNLS) can be protective. Second, it demonstrates the potential benefits of this ligand using an *in vivo* model of acute pancreatitis. Finally, by demonstrating that genetic deletion of RNLS results in more severe experimental pancreatitis, it suggests a role for the endogenous protein in modulating injury. This is further supported by our results showing that inhibition of PMCA4 enhanced secretagogue-stimulated zymogen activation even at subpathologic concentrations.

PMCAs are a widely distributed protein family with four major members that each modulates cellular calcium efflux as well as other signaling pathways (18). PMCA activities and functions are regulated by the lipid environment and subcellular distribution. Variations in isoforms mediate interactions between different PMCAs and distinct scaffolding and signaling pathways. For example, PMCA4b can suppress neuronal NOS and NO generation (19). Work from our laboratory, based on siRNA knockdown, has shown that PMCA4b isoform mediates the protective effects of RNLS in other cell types (7). Here, we show evidence that, in the murine pancreatic acinar cell, PMCA4 immunoreactivity is distributed primarily to the cell's basolateral domain. This finding is consistent with what is found in human pancreas (20). Based on this and the presence of PMCA4b mRNA in murine and human pancreatic acinar cells, we believe that it is also likely an effector for RNLS in pancreatic acinar cells. However, because we also detected PMCA1 mRNA in acinar cells, we cannot exclude it as an RNLS target in this system. We also found that RNLS prevented acinar cell injury and that chemical inhibition of PMCA with caloxin 1b1 blocked this protective effect of RNLS on cell injury. In addition, we found that treatment with caloxin 1b1 enhanced both CER- and carbachol-stimulated zymogen activation. This suggests that activation of PMCA4 by RNLS or other mechanisms can reduce acinar cell injury. This, along with our observation that plasma levels of RNLS dramatically fall with CER treatment, suggests that the loss of circulating RNLS may modulate disease severity. PMCA activation can affect calcium efflux as well as other signaling pathways, including Akt, ERK, NO, and cAMP levels (4). Which of these pathways is linked to the protective effects of RNLS and whether RNLS has important interactions with other plasma membrane proteins are important topics for future study.

In vivo studies using the CER model of acute pancreatitis showed that administration of exogenous recombinant RNLS reduced the severity of cerulein pancreatitis when given after disease onset. Although we demonstrated that RNLS can reduce acute injury to acinar cells, its effectiveness when given after disease onset could reflect its action on the acinar cell as well as other cell types, including inflammatory cells. For example, our published and preliminary studies suggest that RNLS can suppress innate immune responses in macrophages, a cell population that has been shown to mediate injury in acute pancreatitis (6).[4]

[4] G. V. Desir, unpublished observations.

Observations made in these animal and cellular models could be relevant to human disease. For example, that the RNLS$^{-/-}$ mouse develops more severe pancreatitis suggests that deficiency of this protein in humans could increase the severity of acute injury. In this context, RNLS was discovered as a circulating protein that largely disappears in subjects with renal failure. Renal failure is associated with a greater risk of both developing acute pancreatitis and experiencing more severe disease. It is possible that RNLS deficiency contributes to the pancreatitis risk in renal failure. The reduced RNLS levels early in the course of experimental pancreatitis could also account for the benefit of giving exogenous RNLS. Functional polymorphisms in RNLS have been linked to hypertension in humans. It will be of interest to know whether similar variations in this protein can modulate the severity of acute injury, including acute pancreatitis.

In summary, we have shown that the recently described plasma protein RNLS reduces acute pancreatitis injury in cellular and *in vivo* murine models of this disease and that genetic deletion of RNLS led to more severe pancreatitis. An important target for this protective effect is likely the activation of PMCA4b on the pancreatic acinar cell. Our results suggest that RNLS may act through PMCA4 to prevent cell injury associated with pancreatitis and provide initial data suggesting that RNLS could serve as a treatment of acute disease.

Experimental procedures

Ethics statement

All experiments and procedures using animals were approved by the Veterans Administration Institutional Animal Care and Use Committee, West Haven, CT (Veterans Administration Public Health and Safety, Office of Laboratory Animal Welfare Assurance Number A4363-01).

Animals used

All wild-type animals used were male C57/BL6 mice weighing approximately 25 g. The renalase KO mice are on a C57/BL6 background, and both male and female animals used due to availability (8).

Preparation and isolation of recombinant renalase

The gene encoding human renalase1 (hRNLS) was purchased from Enzymax and cloned into pET-28a(+) expression vector (Novagen) to incorporate an N-terminal His tag. BL21 cells (Novagen) were transfected and grown in LB medium containing 100 μg/ml kanamycin. Once cultures reached an OD of 1, isopropyl 1-thio-β-D-galactopyranoside (0.1 mM final) was added to induce protein production. Cultures were grown overnight with shaking at room temperature to avoid the formation of inclusion bodies, the following day bacteria were centrifuged at 4000 $\times$ *g* for 30 min, and the resulting bacterial pellet was collected. The pellet was then solubilized, and recombinant protein was purified using a HisTALON kit (Clontech). 1-ml fractions were collected, and those containing renalase were pooled. Endotoxin was removed from the pooled fractions using endotoxin removal resin according to the manufacturer's directions (Pierce High-capacity Endotoxin Removal Resin, Thermo Scientific, Rockford, IL). The endotoxin-cleared sample was then dialyzed (Slide-A-Lyzer, 10,000 molecular weight cutoff, Thermo Scientific, Rockford, IL) in 2 liters of phosphate-buffered saline (PBS; pH 7.4), changing twice. Dialyzed protein was concentrated with an Amicon Ultra-15 (10,000 molecular weight cutoff, EMD/Millipore, Billerica, MA). Protein concentration was determined using $A_{280\ nm}$, and sample was diluted to 0.5 mg/ml with PBS and stored at −80 °C.

Preparation of isolated pancreatic lobules and pancreatic acini

C57/BL6 or renalase knock-out mice (renalase$^{-/-}$) weighing ~25 g were used to generate pancreatic lobules. On the day of the experiment, animals were euthanized by CO_2 inhalation, and the pancreas was removed. For lobules, pancreatic fragments (~5-mm diameter) were mechanically separated and washed with incubation buffer (10 mM Hepes (pH 7.4), 95 mM NaCl, 4.7 mM KCl, 0.6 mM $MgCl_2$, 1 mM NaH_2PO_4, 10 mM glucose, 2 mM glutamine, 0.1% bovine serum albumin, and 1× minimum essential medium amino acids (Gibco). One to two lobules were then placed into each well of a 24-well Falcon tissue culture plate (BD Biosciences) containing 0.5 ml of incubation medium. For pancreatic acini, the removed pancreas was minced and processed by mechanical disruption and collagenase digestion as described (21). Acini were placed in the incubation buffer above and processed for pancreatitis responses as described (21). All reagents were purchased from Sigma unless otherwise noted.

Induction of pancreatitis in pancreatic lobules and pretreatment with renalase and/or caloxin 1b1

Lobules were pretreated with RNLS (5–25 μg/ml) prior to the induction of pancreatitis by one of the following secretagogues for 30 min to 2 h (depending on the experiment) with either CER (0.1–100 nM), carbachol (1 μM–1 mM), or taurolithocholic acid sulfate (TLCS; 500 μM) to induce pancreatitis responses. RNLS (1–25 μg/ml of medium) was added to appropriate wells 30 min prior to the addition of CER, carbachol, or TLCS. Caloxin 1b1 (100 μM) was used to inhibit PMCA activation and was added to appropriate wells 30 min prior to the addition of RNLS. After treatments, 50 μl of cell-free medium was removed to assay for amylase secretion. The remaining medium containing the pancreatic lobules was homogenized by hand using 10 strokes in a 2-ml glass Teflon homogenizer. The homogenate was centrifuged at 500 $\times$ *g* for 10 min, and the resulting supernatant was used to assay zymogen activation and amylase secretion.

Zymogen activation assays

The supernatant from pancreatic lobules was assayed for zymogen activity using fluorogenic substrates as described (21). Briefly, 50 μl of enzyme substrate (40 mM final) (chymotrypsin from Calbiochem; trypsin from Peptides International, Louisville, KY) was added to each well containing 20–50 μl of sample and 400–430 μl of assay buffer (50 mM Tris (pH 8.1), 150 mM NaCl, and 1 mM $CaCl_2$) for a total volume in the well of 500 μl. The plate was then read using a fluorometric plate reader (Flx800, BioTek Instruments, Winooski, VT) at an excitation wavelength of 380 nm and emission wavelength of 440 nm for

20 measurements over 10 min. The slope of the resulting line, which represents enzyme activity of the homogenate, was normalized to total amylase content.

In vivo model of pancreatitis and renalase post-treatment

Mice (~25 g) were fasted overnight and then given six hourly i.p. injections of cerulein (50 μg/kg of body weight in 200 μl of PBS) to induce pancreatitis. For studies that examined the effects of renalase administration postinduction of pancreatitis, rRNLS (4 mg/kg of body weight in 200 μl of PBS) was given concurrently with the third CER injection. Tissues and blood were collected for assay at relevant time points (all time points are designated as time after first CER injection).

Histology and immunostaining

Pancreatic lobules (*in vitro*) or tissue pieces (*in vivo*) were placed into cassettes and fixed in normal buffered formalin. Specimens were washed into 70% ethanol and brought to the Yale Pathology Tissue Services Lab for paraffin embedding, sectioning, and processing for H&E and immunostaining. Histology slides were examined by light microscopy at 400×, and either histologic markers were scored or immunoreactive cells were counted. Histologic scoring was done based on previously described criteria (22). All histology images were photographed at 400×.

Immunofluorescence

Tissues were removed, cut into small (about 10-mm) cubes, and fixed in 2% paraformaldehyde in PBS for 30 min on ice. Tissues were then washed and placed into 15% sucrose in PBS overnight at 4 °C. The next day tissues were placed into Cryomolds (Sakura Finetek, Torrance, CA) and snap frozen on dry ice in O.C.T. Compound (Sakura Finetek). Thin sections were cut using a cryostat at −20 °C and placed on slides. Samples were permeabilized in IF buffer with Tris-buffered saline (TBS), 0.05% Triton X-100, and 5 mM benzamidine for 5 min × 3 at room temperature followed by a quench/block with IF buffer with 50 mm ammonium chloride and 5% goat serum. Slides were then rinsed in IF buffer twice at room temperature. Primary antibody anti-PMCA4b (JA-3, Santa Cruz Biotechnology, Dallas, TX) was added to slides at a dilution of 1:100 in IF buffer and incubated overnight at 4 °C in a humidified chamber. The next day slides were washed twice with IF buffer with 0.2% BSA for 10 min each followed by washing twice in IF buffer for 10 min each. Second antibody was then added (Alexa Fluor 488 at 1:500 dilution) in IF buffer and incubated at room temperature for 1 h. Thirty minutes into the second antibody incubation phalloidin conjugated to Alexa Flour 555 was added to slides to double label for F-actin during the remaining 30 min. Slides were then washed twice with IF buffer with 0.2% BSA for 5 min each followed by washing twice with IF buffer for 5 min each and finally once with TBS (pH 7.5) for 5 min. Lastly, slides were mounted with VECTASHIELD hard set mounting medium with DAPI (Vector Labs, Burlingame, CA). When dry, slides were examined using a fluorescence microscope (Zeiss Axiophot), and images were captured using a digital camera (Spot Imaging).

Amylase assay

Samples were thawed on ice, and the cell-free supernatant was assayed for secreted amylase. The remaining sample (lobule plus medium) from the zymogen activation assays was assayed for total amylase. Amylase activity was determined using a commercial kit. Amylase secretion was calculated as percent total release (medium/medium + cells). Plasma amylase content was measured according to the manufacturer's instructions (Phaebadas kit, Magle Life Sciences, Lund, Sweden).

PCR

All PCR primers are described in Table 1. The mouse primers for PMCA1–4 (23, 24) and PMCA4a and PMCA4a/b (25) have been described. The human PMCA primers were designed using Primer-BLAST (National Institutes of Health). Human cDNA was provided by Guy Groblewski of the University of Wisconsin. Mouse cDNA was produced from total RNA isolated from mouse pancreatic acini, pancreas, and kidney using TRIzol (Ambion/Thermo Fisher, Grand Island, NY). First-strand cDNA was prepared using a Verso cDNA synthesis kit (Thermo Fisher) following the manufacturer's protocol. PCR was carried out using a Platinum *Taq* DNA polymerase kit (Invitrogen) and 1 μl of first-strand cDNA in a 50-μl reaction volume containing 1× PCR Buffer (from the kit), 1.65 mM $MgCl_2$, 200 mM each deoxynucleotide triphosphate, 1.25 units of *Taq* DNA polymerase (Invitrogen), and 200 nM each primer (Table 1). For amplification of PMCA isoforms, the following conditions were used: initial denaturation for 2 min at 95 °C and then 40 cycles of denaturation (94°, 30 s), annealing (60 °C, 30 s), and extension (72 °C, 30 s). This was followed by a single extension step for 1 min at 72 °C. PCR products were analyzed on 1% agarose gels with ethidium bromide.

MTT assay

The reduction of MTT to formazan is a measure of redox activity and has been used as a marker of cell viability as well as cell proliferation. It is generally thought that this reaction takes place in mitochondria, but a recent study has shown only about 25% of MTT reduction is associated with mitochondria; the remainder takes place at a distance by non-mitochondrial enzymes. This suggests that MTT reduction can be used as a more general marker of redox activity (26). Here, we used MTT reduction to formazan as a general marker of metabolic health. To assay MTT activity, a stock MTT solution (5 mg/ml) was made by dissolving MTT (Invitrogen) in sterile Dulbecco's PBS. The solution was filtered using a 0.2-μm filter unit and stored at −20 °C protected from light. Pancreatic lobules were isolated and treated as indicated above. After 30 min of CER treatment, 100 μl of stock MTT was added to each well (0.45 mg/ml final) for 1 h. Lobules were removed from the wells, blotted dry, and homogenized in 750 μl of buffer (40% dimethylformamide, 2% glacial acetic acid, 16% sodium dodecyl sulfate, and 42% water (pH 4.7)) using a conical tip homogenizer. The homogenate was incubated at 37 °C for 2 h. The homogenate was then centrifuged at 10,000 × *g* for 5 min, and the resulting supernatant was read at 520 nm. Values were normalized to DNA ($A_{260\,nm}$), and activity was expressed as a ratio of MTT (520 nm)/DNA ($A_{260\,nm}$).

Table 1
PCR primers used for determining which PMCA isoforms are present in mouse and human pancreatic acinar cells
F, forward; R, reverse.

Gene	GenBankTM accession number	Primer sequence	Expected size	Refs.
Mouse				
PMCA1	NM_026482	F, 5′-TCT GGC TAC GGA ACC ACC CA-3′ R, 5′-AAA GGC TTC CCG CCA AAC TG-3′	390	4, 9
PMCA2	NM_009723	F, 5′-CAC CCT GCT CTT CGT GGG TG-3′ R, 5′-AGG GAT GGT GGC GAT GAC CT-3′	355	4, 9
PMCA3	NM_177236	F, 5′-ATG AAG AGC TGG CCG AAG GG-3′ R, 5′-GCG TGG TCA GGT AGA TGC CG-3′	345	4, 9
PMCA4	NM_213616	F, 5′-CAA GCC TCT GAT CTC CCC CA-3′ R, 5′-CCA CTG CTC CAT GGT CAG GC-3′	364	4, 9
PMCA4a	NM_001167949	F, 5′-GCA CTG GAT GTG GTG TCT CTT TAT-3′ R, 5′-CAC TCA CTG CCC ACA GGA GGA-3′	417	11
PMCA4a/b	(a) NM_001167949/(b) NM_213616.3	F, 5′-GGA CGA GAT TGA CCT TGC CG-3′ R, 5′-CAC CAT CCA ACA GGA GCA CAC T-3′	(a) 469/(b) 278	11
Human				
PMCA1	NM_001001323.1	F, 5′-AGC ACT GTC TCA GAC CAA CG-3′ R, 5′-AGG AGC ATG CAA AGG AGC AT-3′	555	[a]
PMCA2	NM_001001331.2	F, 5′-GAA ACC GTG CAG GAT TGG TG-3′ R, 5′-GTG AGC TCC AAG AGG TGT CC-3′	179	[a]
PMCA3	NM_021949.3	F, 5′-GCT CTG GTG CCT GTT TGT TG-3′ R, 5′-GAT CTC TTC CTC GCC TTC GG-3′	157	[a]
PMCA4a/b	(a) NM_001001396.2/(b) NM_001684.4	F, 5′-CCG CAA TAC CTA CCC GAT CC-3′ R, 5′-GCA ATC CAC CGC ATT GTT GT-3′	(a) 597/(b) 419	[a]

[a] Primers were designed using Primer-BLAST.

Measurement of edema

Pancreatic tissue was harvested, and its wet weight was determined. Tissues were then dried at 60 °C for at least 48 h and reweighed. Edema was expressed as percent wet weight (wet weight − dry weight/wet weight × 100).

Statistical analysis

Data represent the mean ± S.E. of at least three individual experiments unless otherwise noted with each performed in at least duplicate. Student's *t* test analysis was used to determine statistical significance for *in vitro* experiments, whereas a Mann–Whitney test was used for *in vivo* experiments. A p value of <0.05 was assigned significance.

Author contributions—T. R. K. designed and performed experiments (Figs. 1, 2, and 4–9), analyzed data, prepared figures, and wrote the initial draft of the manuscript. A. M. R. designed and performed experiments (Figs. 1, 4, 5, and 7), analyzed data, and prepared figures. K. D. performed experiments (Fig. 6) and analyzed data. C. S. designed and performed experiments (Fig. 3), analyzed data, and prepared figures. V. P. performed experiments (Figs. 1 and 7–9). S.-L. C. performed experiments (Figs. 1, 7, and 8). G. V. D. designed and produced the renalase knock-out mouse, discussed results, and revised the manuscript. F. S. G. designed experiments, discussed results, and revised the manuscript.

Acknowledgments—We thank Guy E. Groblewski from the University of Wisconsin for providing the human cDNA used for PCR analysis of PMCA isoforms. We also acknowledge the Yale George M. O'Brien Kidney Center at Yale (supported by National Institutes of Health Grant P30DK079310) and the Yale Silvio O. Conte Digestive Diseases Research Core Center (supported by National Institutes of Health Grant P30DK034989) for technical support.

References

1. Peery, A. F., Dellon, E. S., Lund, J., Crockett, S. D., McGowan, C. E., Bulsiewicz, W. J., Gangarosa, L. M., Thiny, M. T., Stizenberg, K., Morgan, D. R., Ringel, Y., Kim, H. P., Dibonaventura, M. D., Carroll, C. F., Allen, J. K., *et al.* (2012) Burden of gastrointestinal disease in the United States: 2012 update. *Gastroenterology* **143,** 1179.e3–1187.e3
2. Gerasimenko, J. V., Gerasimenko, O. V., and Petersen, O. H. (2014) The role of Ca^{2+} in the pathophysiology of pancreatitis. *J. Physiol.* **592,** 269–280
3. Xu, J., Li, G., Wang, P., Velazquez, H., Yao, X., Li, Y., Wu, Y., Peixoto, A., Crowley, S., and Desir, G. V. (2005) Renalase is a novel, soluble monoamine oxidase that regulates cardiac function and blood pressure. *J. Clin. Investig.* **115,** 1275–1280
4. Wang, L., Velazquez, H., Moeckel, G., Chang, J., Ham, A., Lee, H. T., Safirstein, R., and Desir, G. V. (2014) Renalase prevents AKI independent of amine oxidase activity. *J. Am. Soc. Nephrol.* **25,** 1226–1235
5. Guo, X., Hollander, L., MacPherson, D., Wang, L., Velazquez, H., Chang, J., Safirstein, R., Cha, C., Gorelick, F., and Desir, G. V. (2016) Inhibition of renalase expression and signaling has antitumor activity in pancreatic cancer. *Sci. Rep.* **6,** 22996
6. Hollander, L., Guo, X., Velazquez, H., Chang, J., Safirstein, R., Kluger, H., Cha, C., and Desir, G. V. (2016) Renalase expression by melanoma and tumor-associated macrophages promotes tumor growth through a STAT3-mediated mechanism. *Cancer Res.* **76,** 3884–3894
7. Wang, L., Velazquez, H., Chang, J., Safirstein, R., and Desir, G. V. (2015) Identification of a receptor for extracellular renalase. *PLoS One* **10,** e0122932
8. Wu, Y., Xu, J., Velazquez, H., Wang, P., Li, G., Liu, D., Sampaio-Maia, B., Quelhas-Santos, J., Russell, K., Russell, R., Flavell, R. A., Pestana, M., Giordano, F., and Desir, G. V. (2011) Renalase deficiency aggravates ischemic myocardial damage. *Kidney Int.* **79,** 853–860
9. Baggaley, E., McLarnon, S., Demeter, I., Varga, G., and Bruce, J. I. (2007) Differential regulation of the apical plasma membrane Ca^{2+}-ATPase by protein kinase A in parotid acinar cells. *J. Biol. Chem.* **282,** 37678–37693
10. Yang, Y. M., Lee, J., Jo, H., Park, S., Chang, I., Muallem, S., and Shin, D. M. (2014) Homer2 protein regulates plasma membrane Ca^{2+}-ATPase-mediated Ca^{2+} signaling in mouse parotid gland acinar cells. *J. Biol. Chem.* **289,** 24971–24979

11. Lee, H. T., Kim, J. Y., Kim, M., Wang, P., Tang, L., Baroni, S., D'Agati, V. D., and Desir, G. V. (2013) Renalase protects against ischemic AKI. *J. Am. Soc. Nephrol.* **24,** 445–455
12. Li, X., Xie, Z., Lin, M., Huang, R., Liang, Z., Huang, W., and Jiang, W. (2015) Renalase protects the cardiomyocytes of Sprague-Dawley rats against ischemia and reperfusion injury by reducing myocardial cell necrosis and apoptosis. *Kidney Blood Press. Res.* **40,** 215–222
13. Wang, Y., Safirstein, R., Velazquez, H., Guo, X. J., Hollander, L., Chang, J., Chen, T. M., Mu, J. J., and Desir, G. V. (2017) Extracellular renalase protects cells and organs by outside-in signalling. *J. Cell. Mol. Med.* **21,** 1260–1265
14. Roy, N., Chakraborty, S., Paul Chowdhury, B., Banerjee, S., Halder, K., Majumder, S., Majumdar, S., and Sen, P. C. (2014) Regulation of PKC mediated signaling by calcium during visceral leishmaniasis. *PLoS One* **9,** e110843
15. Bruce, J. I., and Elliott, A. C. (2007) Oxidant-impaired intracellular Ca^{2+} signaling in pancreatic acinar cells: role of the plasma membrane Ca^{2+}-ATPase. *Am. J. Physiol. Cell Physiol.* **293,** C938–C950
16. Mankad, P., James, A., Siriwardena, A. K., Elliott, A. C., and Bruce, J. I. (2012) Insulin protects pancreatic acinar cells from cytosolic calcium overload and inhibition of plasma membrane calcium pump. *J. Biol. Chem.* **287,** 1823–1836
17. Samad, A., James, A., Wong, J., Mankad, P., Whitehouse, J., Patel, W., Alves-Simoes, M., Siriwardena, A. K., and Bruce, J. I. (2014) Insulin protects pancreatic acinar cells from palmitoleic acid-induced cellular injury. *J. Biol. Chem.* **289,** 23582–23595
18. Strehler, E. E. (2015) Plasma membrane calcium ATPases: from generic Ca^{2+} sump pumps to versatile systems for fine-tuning cellular Ca^{2+}. *Biochem. Biophys. Res. Commun.* **460,** 26–33
19. Duan, W., Zhou, J., Li, W., Zhou, T., Chen, Q., Yang, F., and Wei, T. (2013) Plasma membrane calcium ATPase 4b inhibits nitric oxide generation through calcium-induced dynamic interaction with neuronal nitric oxide synthase. *Protein Cell* **4,** 286–298
20. Uhlén, M., Fagerberg, L., Hallström, B. M., Lindskog, C., Oksvold, P., Mardinoglu, A., Sivertsson, Å., Kampf, C., Sjöstedt, E., Asplund, A., Olsson, I., Edlund, K., Lundberg, E., Navani, S., Szigyarto, C. A., *et al.* (2015) Proteomics. Tissue-based map of the human proteome. *Science* **347,** 1260419
21. Reed, A. M., Husain, S. Z., Thrower, E., Alexandre, M., Shah, A., Gorelick, F. S., and Nathanson, M. H. (2011) Low extracellular pH induces damage in the pancreatic acinar cell by enhancing calcium signaling. *J. Biol. Chem.* **286,** 1919–1926
22. Wildi, S., Kleeff, J., Mayerle, J., Zimmermann, A., Böttinger, E. P., Wakefield, L., Büchler, M. W., Friess, H., and Korc, M. (2007) Suppression of transforming growth factor β signalling aborts caerulein induced pancreatitis and eliminates restricted stimulation at high caerulein concentrations. *Gut* **56,** 685–692
23. Alexander, R. T., Beggs, M. R., Zamani, R., Marcussen, N., Frische, S., and Dimke, H. (2015) Ultrastructural and immunohistochemical localization of plasma membrane Ca^{2+}-ATPase 4 in Ca^{2+}-transporting epithelia. *Am. J. Physiol. Renal Physiol.* **309,** F604–F616
24. Kim, H. J., Prasad, V., Hyung, S. W., Lee, Z. H., Lee, S. W., Bhargava, A., Pearce, D., Lee, Y., and Kim, H. H. (2012) Plasma membrane calcium ATPase regulates bone mass by fine-tuning osteoclast differentiation and survival. *J. Cell Biol.* **199,** 1145–1158
25. Patel, R., Al-Dossary, A. A., Stabley, D. L., Barone, C., Galileo, D. S., Strehler, E. E., and Martin-DeLeon, P. A. (2013) Plasma membrane Ca^{2+}-ATPase 4 in murine epididymis: secretion of splice variants in the luminal fluid and a role in sperm maturation. *Biol. Reprod.* **89,** 6
26. Bernas, T., and Dobrucki, J. (2002) Mitochondrial and nonmitochondrial reduction of MTT: interaction of MTT with TMRE, JC-1, and NAO mitochondrial fluorescent probes. *Cytometry* **47,** 236–242
27. Shah, A. U., Sarwar, A., Orabi, A. I., Gautam, S., Grant, W. M., Park, A. J., Shah, A. U., Liu, J., Mistry, P. K., Jain, D., and Husain, S. Z. (2009) Protease activation during in vivo pancreatitis is dependent on calcineurin activation. *Am. J. Physiol. Gastrointest. Liver Physiol.* **297,** G967–G973